Korean J. Chem. Eng., **25**(1), 185-189 (2008)

Influence of processing temperature on the image transfer characteristics of an image guide made of polymer optical fibers

Byung-Wook Park, Do-Young Yoon† and Soeun Park

Department of Chemical Engineering, Kwangwoon University, Seoul 139-701, Korea
(*Received 14 September 2007 • accepted 27 October 2007*)

Abstract−An image guide has been made by using polymer optical fibers. Single-strand polymer optical fibers were laid out first in a square array, and the square bundle thus made was fused in a vacuum oven at various processing temperatures. Although the line resolution of an image guide is determined by the number of optical fibers per unit area (i.e., the pixel density), the fusion temperature affects the cohesiveness of neighboring fibers that influences the portrait quality of the image guide. The objective of this study was to investigate the influence of fusion temperature on the portrait quality of the image guide. The image transfer characteristics were evaluated quantitatively by using a computer program that was developed in our laboratory for the comparison with a macrography. The present result indicates that there exists an optimum fusion temperature for the optimum cohesion between neighboring fibers that maximizes the brightness of an image without cross-talk.

Key words: Image Guide, Polymer Optical Fiber, Fusion Temperature, Portrait Quality

INTRODUCTION

The use of optical image guides has been growing rapidly in various medical and industrial applications. Besides endoscopes or videoscopes, optical image guides are indispensable for other medical applications such as Single Photon Emission Computed Tomography (SPECT) and Position Emission Tomography (PET) for X-ray imaging. Nonmedical applications of optical image guides may include boroscopes, cystoscopes, copy machines, and bar code scanners. In addition, the real time X-ray imaging devices for Non-Destructive Examination (NDE) systems are also important applications for product quality control. Demands on design and performance of endoscopic instruments, including very small diameters and extreme flexibility, have increased over the last thirty years.

Fiber-optic endoscopes permit visualization of normally accessible areas within the body and without pain or discomfort for patients. A flexible endoscope is essential because rigid endoscopes have limited use in digestive endoscopies. Nearly all endoscopes include two different types of optical fibers: one for use as an image guide and the other as a light guide. Additionally, ancillary channels may be present for the passage of air, water, as well as remote control implements such as biopsy forceps or cytology brushes. In a flexible endoscope, a bundle of precisely aligned flexible optical fibers is used, while in rigid endoscopes the image is conveyed by a relay of lenses. The classical rigid endoscopes have a number of periscope and field lenses in order to convey the image from distal end to the eyepiece [1]. In some cases, from 40 up to 50 lenses may be used for considerable optical aberration, light loss and ghost images. In addition, off centering of lenses can cause significant vignetting and image deterioration unless great care is taken in system design.

Even though the concept of endoscopy originated in the early 19th century, the first endoscope made of optical fibers (fiberscope) was used for viewing the stomach and esophagus at the University of Michigan School of Medicine in 1957 [2]. Since then, there has been rapid progress in endoscope development. In the 1980's, ultra-thin optical fibers were produced and, as a result, the diameter of an endoscope could be reduced to less than 1 mm. These ultra-thin endoscopes are used to examine very small parts of internal organs. In recent years, ultra-thin silica-based needlescopes have been developed for medical applications such as imaging and clinical diagnosis. The ultra-thin needlescopes contain 2,000 to 6,000 pixels with a diameter of about 0.2 mm to 0.5 mm. It has been found that it is easy to insert these ultra-thin needlescopes into the mammary glands to detect breast cancer at early stages [3]. In addition, this kind of needlescope makes it possible to obtain real-time images of inaccessible locations within the human body [4]. Today, ophthalmic endoscopes allow a direct viewing of certain internal structures of the eye including the back side of the iris and posterior chamber [5]. Ultra-thin fiberscopes used in cardiology, called angioscopes, convey images of heart valves as well as obstructions (plaques) in coronary arteries. Existing flexible medical image guides use glass optical fibers which are intrinsically brittle. Yet very high flexibility is a major requirement for specialized procedures such as examination of the billiard duct. It is inevitable, even in standard procedures, that some glass fibers will be broken in use. Even new unused endoscopes contain broken fibers, which create darkened areas in the image. Deterioration of optical performance due to progressive fiber breakage leads to an endoscope being downgraded to sub-critical work and eventually discarded.

Glass fibers are capable of withstanding strains only up to 0.5-1.5% compared to 13% for PMMA-based Polymer Optical Fiber (POF) [6]. POF image guides are based on PMMA for light transmission, and fluoropolymers for fiber cladding purposes [1]. The image brightness transmitted by the guide depends on the square of the numerical aperture of the guide. As image guides have been made using polymer optical fibers, the fusion temperature for single-strand polymer optical fibers in a square array and the square

†To whom correspondence should be addressed.
E-mail: yoondy@daisy.kw.ac.kr

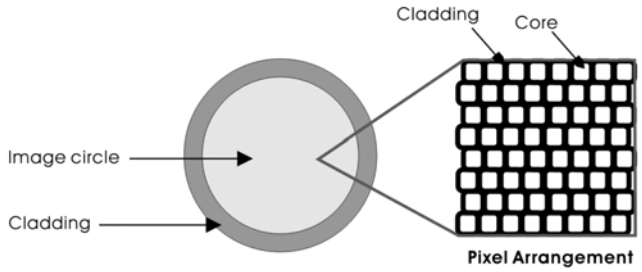

Fig. 1. Schematic structure of endoscope image guide.

bundle are important to determine the line resolution of an image guide by the number of the pixel density. Therefore, this study focuses on investigating the influence of processing variables to optimize the image-guide fusion conditions for the inherent POF characteristics affecting the cohesiveness of neighboring fibers that influences the portrait quality of the image guide.

IMAGE-QUALITY COMPUTATIONS

To transmit an image, a large number of single fibers should be aligned and fused together. This means the assembly of optical fibers in which the fibers are ordered in exactly the same way at both ends of the bundle to create an image. This type of fiber bundle is a coherent bundle or image guide bundle. Fig. 1 shows a schematic of the cross-section of the structure of an image guide composed of optical fibers. For a fiber bundle, the resolution can be defined by about half a line pair per fiber core [7]. Therefore, the optimum conditions for a given desired resolution depend on parameters such as cladding thickness, refractive index of the core and the cladding and the wavelength of the incident ray, and the fabrication process.

Signal-to-noise (SNR) measurements are estimates of the quality of a reconstructed image compared with an original image. The basic idea is to compute a single number that reflects the quality of the reconstructed images. Reconstructed images with higher metrics are judged to be better [8]. In fact, traditional SNR measurements do not equate with human subjective perception. Even though several research groups are working on perceptual measurements, we will use the signal-to-noise measurement, which is much easier to compute.

The actual metric to be computed is the peak signal-to-reconstructed image measurement, which is called PSNR. Let us assume a source image f(i, j) that contains N by N pixels and a reconstructed image F(i, j) where F is reconstructed by decoding the encoded version of f(i, j). Error metrics are computed only on the luminance so that the pixel values f(i, j) range between black (0) and white (255). The mean squared error (MSE) of the reconstructed image is defined as follows:

$$\mathrm{MSE}=\frac{1}{\mathrm{MN}}\sum_{n=1}^{M}\sum_{m=1}^{N}[\hat{g}(n,m)-g(n,m)]^2 \tag{1}$$

where $\hat{g}(n, m)$ and g(n, m) mean the original picture and the compared picture, respectively [9]. As for MSE having sensitive features, the summation should be done over all pixels. The root mean squared error (RMSE) is the square root of MSE. Therefore, the peak signal-to-reconstructed image measurement (PSNR) in decibels (dB) is computed by using

$$\mathrm{PSNR}=-10\log_{10}\frac{\mathrm{MSE}}{S^2}=20\log_{10}\frac{S}{\mathrm{RMSE}} \tag{2}$$

The MPEG committee used an informal threshold of 0.5 dB PSNR to decide whether to incorporate a coding optimization because they believed that an improvement of that magnitude would be visible. Moreover, some definitions of PSNR use 255^2/MSE rather than 255/MSE. The use of either formulation does not matter in the present study because we are interested in the relative comparison, not the absolute values.

The other important technique for displaying error is to construct an error image which shows the pixel-by-pixel errors. The simplest computation of this image is to create an image by taking the difference between the reconstructed pixel and the original one. It is difficult to see these images because the display for zero difference is black. And most of the errors are small numbers because they are affected by the shades of black. The typical construction of the error image multiplies the difference by a constant to increase the visible difference and translates the entire image to a gray level [10]. The computation is as follows:

$$E(i, j)=2[f(i, j)-F(i, j)]+128 \tag{3}$$

where E(i, j) denotes the pixel-by-pixel error. In order to investigate the portrait characteristic of the image guide in the present study, the manufacturing image guide using POF has been performed simultaneously.

EXPERIMENTATION AND RESULTS

1. Manufacturing of POF Image Guide

Commercially available POF based on high-purity MMA (Methyl Methacrylate, 99%) and BzMA (Benzyl Methacrylate) co-polymers was prepared from a domestic company (Optimedia Inc. Ltd., Sungnam). Measurements of the light transmission of the fibers were performed by the conventional cut-back method using an optical power meter (Anritsu, ML9002A). The results are shown in Fig. 2 for the case of the 1mm fibers. These data show a fundamental advantage for the current use of the POF.

The manufacturing procedures of the POF image guide begin

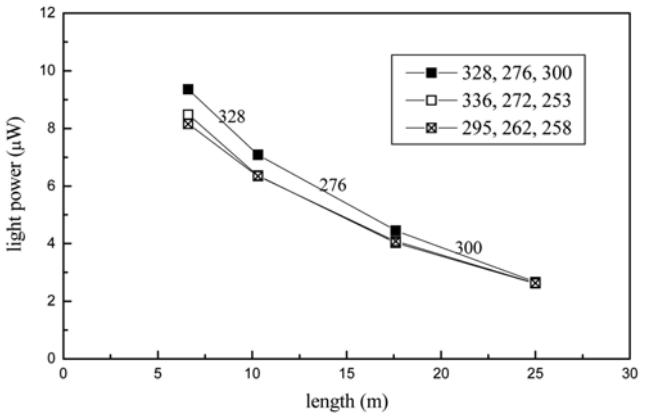

Fig. 2. Attenuation measurements of POF produced by Optimedia, Inc.

with image block equipment that was manufactured by Al units (20×20×250 mm, anodized) that were designed by us. It was very difficult to handle the strand-POF layout in the image block frame; however, the exact arrangement for the POF image block was endeavored during the layout. It was possible to make polar and parallel coordinates of pixels. All inner walls of the Al units were covered by Teflon sheet (3 M). After the arrangement of polymer optical fibers in the image block frame, the POF bundle in the frame was fused during the molding process. Molding process was built by using a vacuum chamber (JeoTech, OV-02) maintained at a PID-controlled set temperature. In the vacuum chamber, it was kept at the pressure of 10^{-3}-10^{-4} torr during 24 hours at a specified temperature.

2. Effect of Fusion Temperature on POF Image Guides

During the molding process, the fusion temperature was varied in order to estimate the portrait characteristics of the image bundle before thermal drawing. The temperature in the vacuum chamber, i.e., the fusion temperature, was fixed at a constant temperature ranging from 110 °C to 130 °C. The fusion temperature is very important for characterizing the external and internal shapes of the bundle of POF. Below 110 °C as a fusion temperature, many poor pixels were observed. It is considered that it was not perfect to mold a POF bundle at the low temperature region below 110 °C. On the other hand, unexpected bubbles appeared at higher temperature conditions above 130 °C. The glass transition temperature of POF is considered to be affected to swell the POF within the bundle. Therefore, the higher temperature is not proper for the molding process. These bounds of temperature were useful for the molding process that was done in our experiment. The available range of temperature for a better quality of portrait can be determined from 115 °C to 125 °C. The original pictures for 3 characters of "P", "B", and "W" were compared with the guided images through image guides molded at different fusion temperatures, as shown in Fig. 3.

Table 1 represents the number of pixels for poor image per square area with respect to the fusion temperature. We observed the transferred image of the fused image-guide bundle and counted the number of poor pixel images per square area at the experiment temperature manually. It can be found that the number of poor pixel images

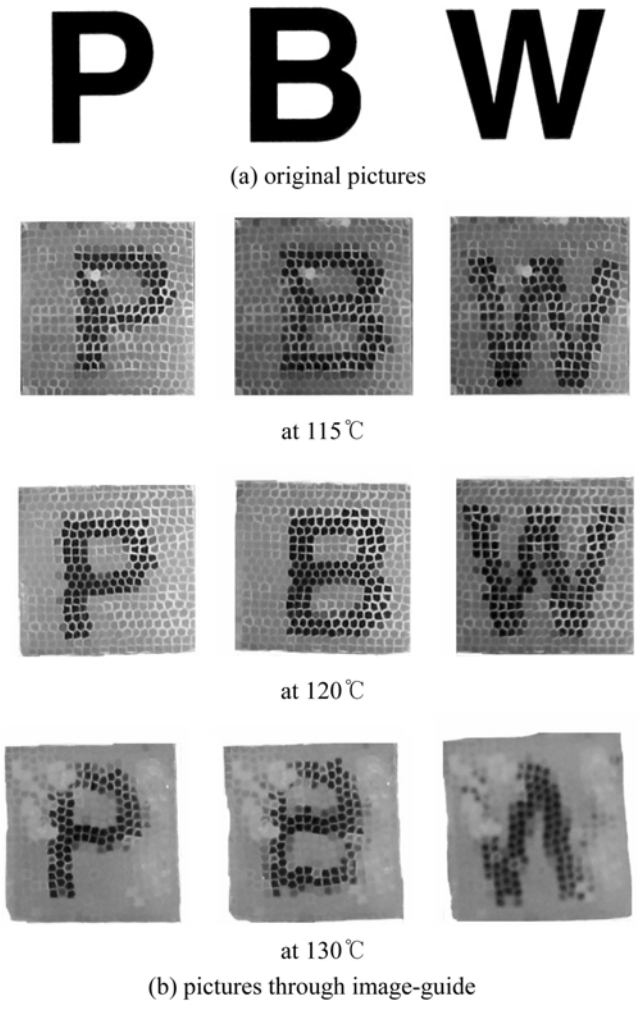

Fig. 3. Comparison of original pictures with guided ones at different fusion temperatures.

Table 1. Change of poor pixel number per square at different fusion temperatures

Fusion temperature (°C)	115	117.5	120	122.5	125	127.5	130
Number of poor pixels	20	12	3	10	30	41	94

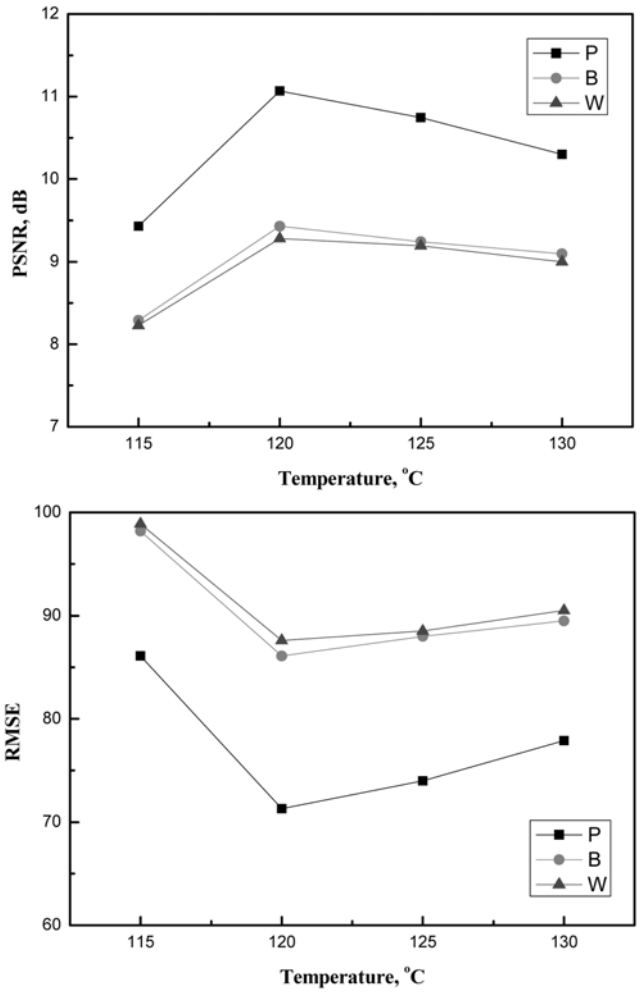

Fig. 4. PSNR and RMSE with respect to the fusion temperature.

at 120 ºC was 3, which was the minimum value relative to the different temperature conditions. The number of poor pixel images was increased slowly with decreasing temperature below 120 ºC and rapidly with increasing temperature above 120 ºC. For this reason, the optimal process temperature can be proposed to be around 120 ºC among present different fusion temperatures. In addition to the macrography providing the raw count distribution of the input pixel image, a quantitative evaluation needs to be given that can be used usually in image-quality computations.

3. Evaluation of Portrait Quality for Image Transfer

Here is introduced an estimating portrait characteristic method both PSNR (Peak Signal-to-Noise Ratio) and MSE (Mean-Squared Error), where computational methods in portrait characteristics are used. In order to evaluate the feasibility of the method of objective measurement with numerical principle of image guide quality, the observant condition was of unrelated observers, respectively. This measurement equipment consists of a digital camera, an image guide and ramps. The distance between camera and image was 200 mm for taking a picture and many of ramps were used to minimize showdown effect.

Fig. 4 shows the portrait quality for image transfer at the different fusion temperature. It was plotted in terms of RMSE and PSNR explained earlier. For these calculations, we have written a simple program for estimating portrait quality by using Visual Basic and C++. Its user interface is shown in Fig. 5(a). The right windows of Fig. 5(a) are for setting initial conditions and it helps the operator in choosing the situation for comparison. The left side of the window displays the pictures and information of histograms such as color distributions. They are computed automatically by the speed modulation algorithm where the Random Noise Average (RNA) meth-

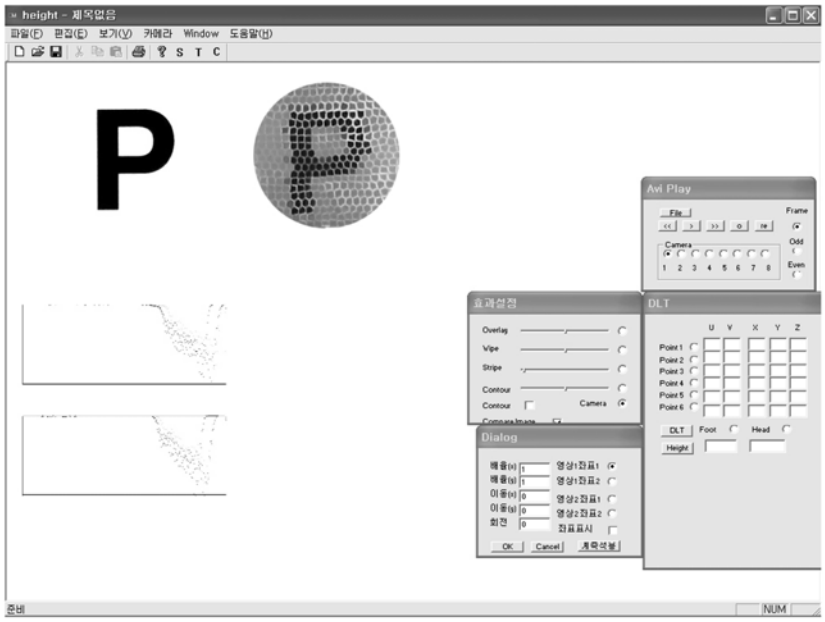

(a) user interface

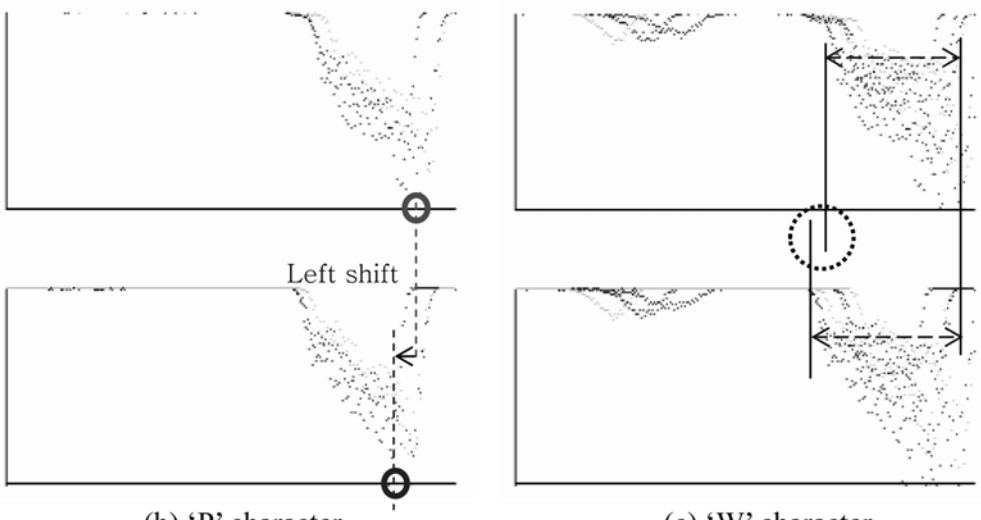

(b) 'P' character (c) 'W' character

Fig. 5. Histograms of 'P' and 'W' characters at 120 ºC.

od is applied. The RNA function code compares a large number of pictures from a camera for elimination of noise. As shown in the figure, the portrait through the image guide is shown in a circle because we used a method of abstracting outlines. It is possible to compare exactly the original with image guide portrait for accurate position of the XY-axis. The maximum value of PSNR (dB) and the minimum one of PMSE for all three characters (P, B and W) were found at our optimal process temperature of 120 °C. It is interesting that the results from the manual count of poor pixels are identical to those from the image-computation technique using a computer.

In addition to providing quantitative information of the portrait quality, our program also gives the corresponding histogram that each frequency appears in the spectrum. Fig. 5 shows the histograms of 'P' and 'W' characters at 120 °C. The upper part is the original picture and the lower part is a portrait of the image guide. Also, the x-axis and y-axis denote the brightness and the frequency of color, respectively. We obtained nearly similar results from histograms of the present characters. But, the histogram of the picture through an image guide had a tendency of the left shift of a peak position. And the area of a histogram distribution along the frequency became larger than that of the original picture. These tendencies mean that the picture through image guide seems to be dark. And also, the distribution of color becomes much broader. This is the evidence that there are bad pixels in the image guide. The present program provides other information for scattering and dispersing images for some special color, which can be used originally in estimating digital images as a value to judge the portrait quality.

CONCLUSION

In this study we have shown that the optimal fusion temperature is very important to transmit light and images through developing the new portrait characteristic method for image guides. A few of previous estimating portrait characteristics of monitors and TV for good quality seem to have difficulty comparing between monitors, because many electric signals need to be solved in comparing methods. The developed method using objective comparing method almost perfectly fits some images and portraits without an understanding of the electric signal process. Most of all, it is interesting to evaluate many image data quantitatively with a histogram describing the distribution of color of some special material and transmit rate. We hope that the present studies will be helpful in other developments of manufacturing of image and light guides.

ACKNOWLEDGMENTS

This work was supported under the research grant from Korea Research Foundation (KRF-2003-041-D00164). The authors also would like to thank Optimedia, Inc., for the supply of polymer optical fibers.

REFERENCES

1. F. Suzuki, *SPIE*, **1592**, 150 (1991).
2. B. I. Hirschowitz, *Gastrology*, **764**, 864 (1979).
3. Y. Hong and J. Ku, *Polymer Science Technology*, **13**, 187 (2002).
4. L. S. Kiat, K. Tanaka, T. Tsumanuma and K. Sanada, *SPIE*, **1649**, 208 (1992).
5. P. O. Rol, R. Jenny, D. Beck, F. Fankhauser and P. Niederer, *Optical Engineering*, **34**, 2070 (1995).
6. S. H. Im, D. J. Suh, O. O. Park, H. Cho, J. S. Choi, J. K. Park and J. T. Hwang, *Korean J. Chem. Eng.*, **19**, 505 (2002).
7. C. Yeh, *Handbook of fiber optics theory and application*, Academic Press, New York (1990).
8. A. N. Netravali and B. G. Haskell, *Digital pictures: Representation, compression*, standards (2nd ed.), Plenum Press, New York, NY (1995).
9. T. Y. Chung, *Trans. KIEE*, **48A**, 1589 (1999).
10. M. Rabbani and P. W. Jones, *Digital image compression techniques*, SPIE Optical Engineering Press, Bellevue, Washington, Vol TT7 (1991).